Electronic Supplementary Material (ESI) for CrystEngComm.
This journal is © The Royal Society of Chemistry 2023

Dinuclear and Trinuclear Cyano-Bridged {$Dy^{III}M^{IV}$} (M = W, Mo) Single-Molecule Magnets Supported by Pentadentate Schiff-Base ligands

Pan-Dong Mao,[a] Hui-Ying Sun,[a] Fei-Fei Yan,[a] Shi-Hui Zhang,[a] Xin-Feng Li,[a] Ren-He Zhou,[a] Yi-Quan Zhang,[b] Yin-Shan Meng*[a] and Tao Liu*[a]

[a.] State Key Laboratory of Fine Chemicals, Frontier Science Center for Smart Materials, School of Chemical Engineering, Dalian University of Technology, Dalian 116024, China

[b.] Jiangsu Key Lab for NSLSCS, School of Physical Science and Technology, Nanjing Normal University, Nanjing 210023, China

*Corresponding author. Email: mengys@dlut.edu.cn; liutao@dlut.edu.cn

CONTENTS

Table S1. Crystallographic data and structure refinements for complexes **1**−**4**.

Complexes	**1**	**2**	**3**	**4**
Formula	$C_{50}H_{64}N_{22}O_{18}Dy_2W$	$C_{50}H_{64}N_{22}O_{18}Dy_2Mo$	$C_{29}H_{48}N_{15}O_{16.5}DyW$	$C_{31}H_{39}N_{15}O_{16.5}DyMo$
T	120 K	120 K	120 K	120 K
F_W	1770.08	1682.17	1217.17	1144.21
Crystal system	Monoclinic	Monoclinic	Triclinic	Triclinic
Space group	$C2/c$	$C2/c$	$P\bar{1}$	$P\bar{1}$
a (Å)	27.0713(11)	26.9939(9)	10.4246(11)	10.5532(9)
b (Å)	9.5260(3)	9.5351(3)	11.7295(11)	11.6027(10)
c (Å)	24.0085(10)	24.0996(7)	18.7320(19)	18.7684(16)
α (˚)	90	90	93.031(3)	92.524(2)
β (˚)	93.820(4)	93.714(3)	95.698(3)	95.871(2)
γ (˚)	90	90	108.135(3)	108.109(2)
V (Å^3)	6177.6(4)	6190.0(3)	2157.4(4)	2165.8(3)
Z	4	4	2	2
ρ_{calc} (mg/m^3)	1.903	1.805	1.874	1.755
F (000)	3472.0	3344.0	1198.0	1140.0
Reflections collected	25571	8872	75085	55238
Unique reflections (R_{int})	0.0557		0.0456	0.0439
Goodness–of–fit on F^2	1.059	0.866	1.081	1.046
R_1 [I>2σ(I)][a]	0.0406	0.0426	0.0378	0.0365
wR_2 [I>2σ(I)][b]	0.0819	0.1000	0.0847	0.0870

[a]$R_1 = \Sigma(|F_o|-|F_c|)/\Sigma|F_o|$, [b]$wR_2 = \{\Sigma[w(F_o^2-F_c^2)^2]/\Sigma[w(F_o^2)^2]\}^{1/2}$

Table S2. Selected bond lengths (Å) and bond angles (˚) for complex **1**.

Complex 1$^{120\ K}$			
Bond length (Å)			
Dy1–N4	2.482(5)	Dy1–O2	2.404(3)
Dy1–N7	2.596(4)	Dy1–O3	2.345(3)
Dy1–N8	2.575(4)	Dy1–O4	2.405(3)
Dy1–N9	2.529(4)	Dy1–O5	2.339(3)
Dy1–O1	2.475(3)		
Bond angle (°)			
N4–Dy1–N7	64.46(14)	O3–Dy1–N8	124.62(12)
N4–Dy1–N8	86.41(15)	O3–Dy1–N9	63.71(12)
N4–Dy1–N9	129.71(15)	O3–Dy1–O1	101.96(11)
N8–Dy1–N7	60.26(12)	O3–Dy1–O2	70.17(11)
N9–Dy1–N7	118.05(12)	O3–Dy1–O4	81.05(12)
N9–Dy1–N8	61.51(13)	O3–Dy1–O5	77.74(12)
O1–Dy1–N4	80.69(14)	O4–Dy1–N4	73.20(14)
O1–Dy1–N7	61.64(18)	O4–Dy1–N7	125.28(13)
O1–Dy1–N8	120.33(11)	O4–Dy1–N8	84.92(12)
O1–Dy1–N9	148.12(12)	O4–Dy1–N9	66.73(12)
O2–Dy1–N4	71.26(14)	O4–Dy1–O1	142.43(11)
O2–Dy1–N7	117.81(11)	O5–Dy1–N4	139.53(14)
O2–Dy1–N8	153.92(13)	O5–Dy1–N7	76.66(12)
O2–Dy1–N9	123.66(12)	O5–Dy1–N8	83.76(13)
O2–Dy1–O1	70.22(11)	O5–Dy1–N9	77.95(12)
O2–Dy1–O4	76.00(12)	O5–Dy1–O1	70.99(11)

O3–Dy1–N4	137.62(13)	O5–Dy1–O2	121.98(13)
O3–Dy1–N7	153.09(13)	O5–Dy1–O4	144.11(11)

Table S3. Selected bond lengths (Å) and bond angles (˚) for complex **2**.

Complex 2$^{120\ K}$			
Bond length (Å)			
Dy1–N4	2.491(8)	Dy1–O2	2.417(5)
Dy1–N7	2.599(7)	Dy1–O3	2.351(5)
Dy1–N8	2.572(6)	Dy1–O4	2.402(5)
Dy1–N9	2.525(6)	Dy1–O5	2.337(5)
Dy1–O1	2.474(5)		
Bond angle (°)			
N4–Dy1–N7	64.6(2)	O3–Dy1–N8	124.60(19)
N4–Dy1–N8	87.0(2)	O3–Dy1–N9	63.6(2)
N4–Dy1–N9	130.6(2)	O3–Dy1–O1	101.92(18)
N8–Dy1–N7	64.6(2)	O3–Dy1–O2	70.54(18)
N9–Dy1–N7	118.1(2)	O3–Dy1–O4	81.38(19)
N9–Dy1–N8	61.5(2)	O3–Dy1–O5	77.83(19)
O1–Dy1–N4	80.0(2)	O4–Dy1–N4	73.3(2)
O1–Dy1–N7	61.70(19)	O4–Dy1–N7	124.9(2)
O1–Dy1–N8	120.71(18)	O4–Dy1–N8	84.3(2)
O1–Dy1–N9	148.0(2)	O4–Dy1–N9	66.9(2)
O2–Dy1–N4	70.0(2)	O4–Dy1–O1	142.39(18)
O2–Dy1–N7	117.73(19)	O5–Dy1–N4	139.4(2)
O2–Dy1–N8	152.9(2)	O5–Dy1–N7	76.6(2)
O2–Dy1–N9	123.65(19)	O5–Dy1–N8	84.0(2)
O2–Dy1–O1	70.55(17)	O5–Dy1–N9	77.7(2)
O2–Dy1–O4	75.63(19)	O5–Dy1–O1	71.15(18)

O3–Dy1–N4	137.2(2)	O5–Dy1–O2	122.8(2)
O3–Dy1–N7	153.1(2)	O5–Dy1–O4	144.18(18)

Table S4. Selected bond lengths (Å) and bond angles (˚) for complex **3**.

Complex 3$^{120\ K}$			
Bond length (Å)			
Dy1–N8	2.462(4)	Dy1–O2	2.454(4)
Dy1–N11	2.619(5)	Dy1–O3	2.353(4)
Dy1–N12	2.602(4)	Dy1–O4	2.394(4)
Dy1–N13	2.553(4)	Dy1–O5	2.313(4)
Dy1–O1	2.411(4)		
Bond angle (°)			
N8–Dy1–N11	66.03(15)	O3–Dy1–N13	63.13(13)
N8–Dy1–N12	87.71(15)	O3–Dy1–O1	105.62(12)
N8–Dy1–N13	131.93(14)	O3–Dy1–O2	65.68(12)
N12–Dy1–N11	59.68(14)	O3–Dy1–O4	79.73(13)
N13–Dy1–N11	116.11(14)	O4–Dy1–N8	71.81(14)
N13–Dy1–N12	61.12(14)	O4–Dy1–N11	125.05(13)
O1–Dy1–N8	75.90(14)	O4–Dy1–N12	85.69(13)
O1–Dy1–N11	61.69(13)	O4–Dy1–N13	70.32(13)
O1–Dy1–N12	120.82(13)	O4–Dy1–O1	137.00(13)
O1–Dy1–N13	150.67(13)	O4–Dy1–O2	79.76(13)
O1–Dy1–O2	65.20(13)	O5–Dy1–N8	139.05(14)
O2–Dy1–N8	75.82(14)	O5–Dy1–N11	76.60(14)
O2–Dy1–N11	119.90(14)	O5–Dy1–N12	87.55(14)
O2–Dy1–N12	160.73(13)	O5–Dy1–N13	79.09(13)
O2–Dy1–N13	123.95(13)	O5–Dy1–O1	71.94(12)
O3–Dy1–N8	135.39(14)	O5–Dy1–O2	111.44(13)

O3–Dy1–N11	154.55(13)	O5–Dy1–O3	78.43(14)
O3–Dy1–N12	124.10(14)	O5–Dy1–O4	148.06(13)

Table S5. Selected bond lengths (Å) and bond angles (˚) for complex **4**.

Complex 4$^{120\ K}$			
Bond length (Å)			
Dy1–N8	2.463(3)	Dy1–O2	2.447(3)
Dy1–N11	2.614(3)	Dy1–O3	2.359(3)
Dy1–N12	2.591(3)	Dy1–O4	2.395(3)
Dy1–N13	2.549(3)	Dy1–O5	2.322(3)
Dy1–O1	2.411(3)		
Bond angle (°)			
N8–Dy1–N11	66.39(11)	O3–Dy1–N13	63.08(10)
N8–Dy1–N12	86.92(11)	O3–Dy1–O1	105.57(9)
N8–Dy1–N13	131.42(11)	O3–Dy1–O2	66.00(10)
N12–Dy1–N11	59.70(10)	O3–Dy1–O4	80.11(10)
N13–Dy1–N11	115.75(11)	O4–Dy1–N8	71.62(11)
N13–Dy1–N12	61.10(10)	O4–Dy1–N11	125.00(10)
O1–Dy1–N8	76.24(11)	O4–Dy1–N12	84.72(10)
O1–Dy1–N11	61.92(10)	O4–Dy1–N13	70.00(10)
O1–Dy1–N12	121.20(10)	O4–Dy1–O1	137.23(10)
O1–Dy1–N13	150.82(10)	O4–Dy1–O2	79.55(10)
O1–Dy1–O2	65.59(10)	O5–Dy1–N8	139.28(11)
O2–Dy1–N8	75.79(11)	O5–Dy1–N11	76.24(10)
O2–Dy1–N11	120.42(10)	O5–Dy1–N12	87.91(10)
O2–Dy1–N12	159.54(11)	O5–Dy1–N13	78.97(10)
O2–Dy1–N13	123.80(10)	O5–Dy1–O1	72.22(10)
O3–Dy1–N8	135.79(11)	O5–Dy1–O2	112.32(10)

O3–Dy1–N11	154.06(11)	O5–Dy1–O3	78.25(10)
O3–Dy1–N12	124.06(10)	O5–Dy1–O4	147.77(10)

Table S6. Selected intra- and intermolecular distances and angles for complexes **1**−**4**.

angles (°)	**1**	**2**	**3**	**4**
Dy1–M1–Dy1a	145.18	144.71		
Dy1–N4–C4	160.72	160.97		
Dy1–N8–C8			148.98	149.07
The intramolecular distances between the centre atoms (Å)				
Dy1···Dy1a	10.834	10.838		
Dy1–M1	5.673	5.672	5.541	5.539
The shortest intermolecular Dy···Dy distances (Å)				
Dy···Dy	7.272	7.251	7.257	7.267
Intermolecular π···π (Å) contacts				
$\pi_{pyridyl}\cdots\pi_{pyridyl}$ (red)	3.927	3.890	3.689	3.702

M = W, Mo

Table S7. SHAPE analyses of Dy^{III} in complexes **1**−**4**.

EP (D_{9h}): Enneagon; OPY (C_{8v}): Octagonal pyramid; HBPY (D_{7h}): Heptagonal bipyramid; JTC (C_{3v}): Johnson triangular cupola J3; JCCU (C_{4v}): Capped cube J8; CCU (C_{4v}): Spherical-relaxed capped cube; JCSAPR (C_{4v}): Capped square antiprism J10; CSAPR (C_{4v}): Spherical capped square antiprism; JTCTPR (D_{3h}): Tricapped trigonal prism J51; TCTPR (D_{3h}): Spherical tricapped trigonal prism; JTDIC (C_{3v}): Tridiminished icosahedron J63; HH (C_{2v}): Hula-hoop; MFF (Cs): Muffin.

	EP (D_{9h})	OPY (C_{8v})	HBPY (D_{7h})	JTC (C_{3v})	JCCU (C_{4v})	CCU (C_{4v})	JCSAPR (C_{4v})
1_Dy	31.066	23.086	15.742	14.976	6.765	5.659	4.030
	CSAPR (C_{4v})	JTCTPR (D_{3h})	TCTPR (D_{3h})	JTDIC (C_{3v})	HH (C_{2v})	MFF (C_s)	
	3.056	3.198	3.026	13.093	6.512	2.798	

	EP (D_{9h})	OPY (C_{8v})	HBPY (D_{7h})	JTC (C_{3v})	JCCU (C_{4v})	CCU (C_{4v})	JCSAPR (C_{4v})
2_Dy	31.198	23.040	15.761	15.126	6.818	5.685	3.972
	CSAPR (C_{4v})	JTCTPR (D_{3h})	TCTPR (D_{3h})	JTDIC (C_{3v})	HH (C_{2v})	MFF (C_s)	
	2.990	3.194	2.985	12.979	6.550	2.679	

	EP (D_{9h})	OPY (C_{8v})	HBPY (D_{7h})	JTC (C_{3v})	JCCU (C_{4v})	CCU (C_{4v})	JCSAPR (C_{4v})
3_Dy	31.248	21.765	15.131	15.653	6.944	5.799	4.705
	CSAPR (C_{4v})	JTCTPR (D_{3h})	TCTPR (D_{3h})	JTDIC (C_{3v})	HH (C_{2v})	MFF (C_s)	
	3.706	3.970	4.177	12.359	4.877	2.983	

	EP (D_{9h})	OPY (C_{8v})	HBPY (D_{7h})	JTC (C_{3v})	JCCU (C_{4v})	CCU (C_{4v})	JCSAPR (C_{4v})
4_Dy	31.454	21.865	15.234	15.621	7.057	5.905	4.536
	CSAPR (C_{4v})	JTCTPR (D_{3h})	TCTPR (D_{3h})	JTDIC (C_{3v})	HH (C_{2v})	MFF (C_s)	
	3.520	3.883	3.997	12.451	4.981	2.859	

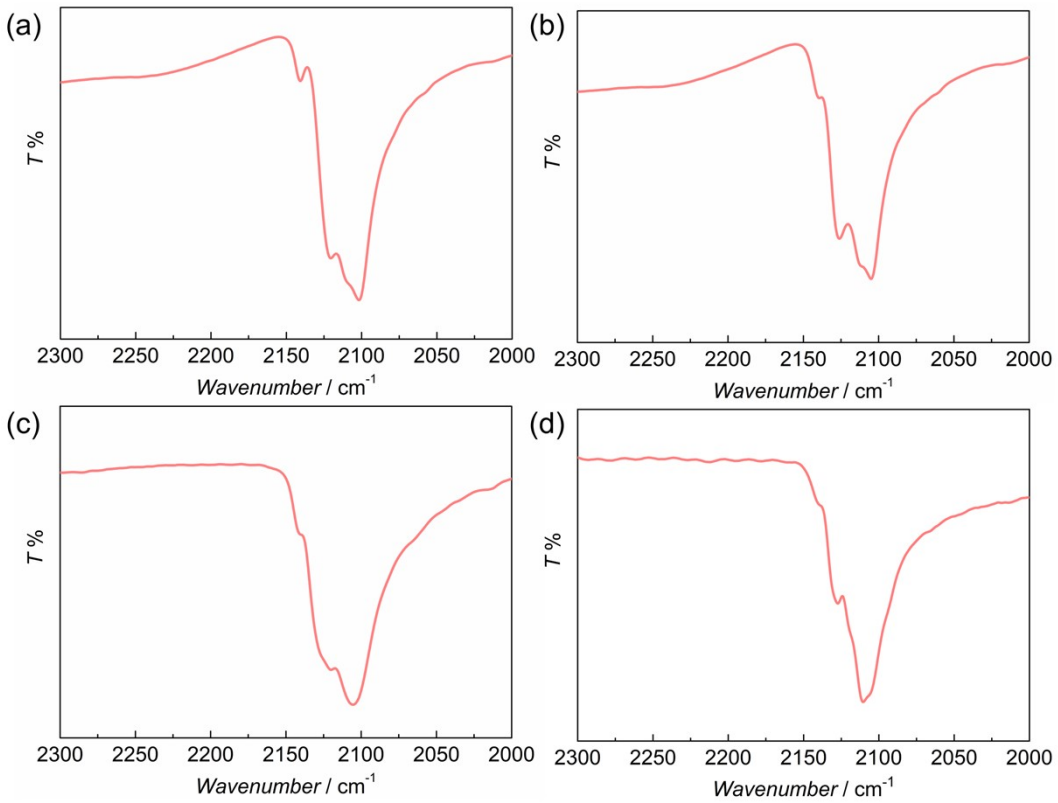

Fig. S1 The IR spectra of complexes **1** (a)−**4** (d) at the range of 2000−2300 cm^{-1}.

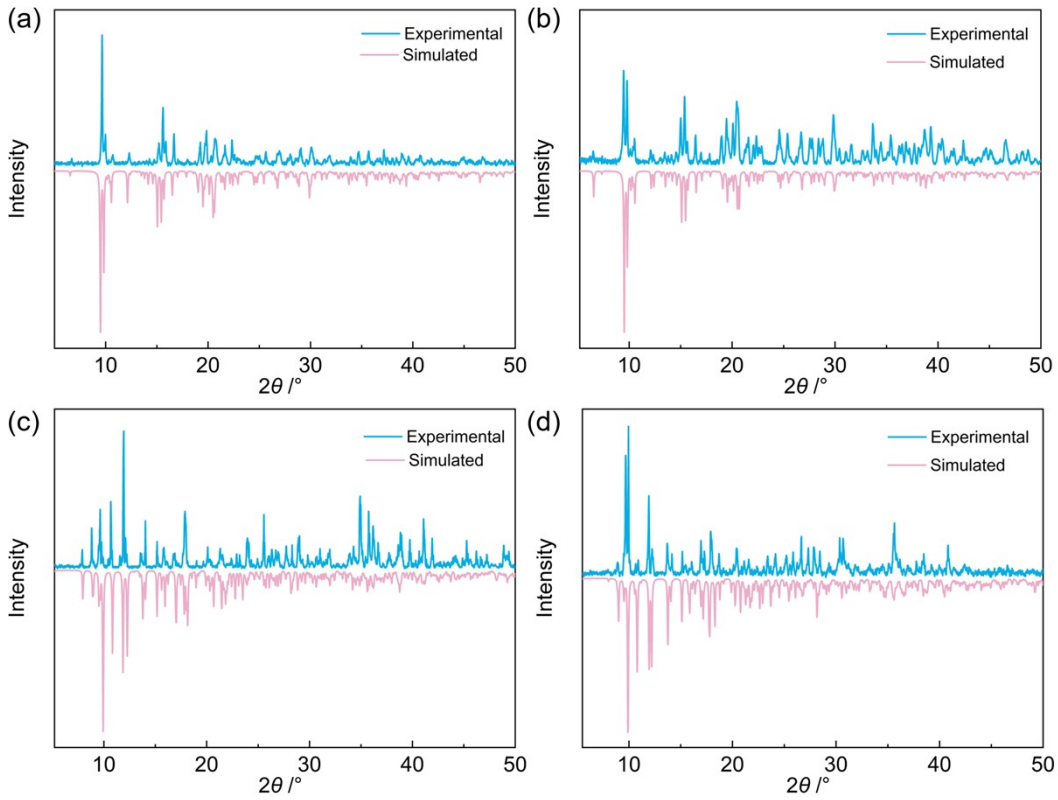

Fig. S2 Powder-XRD diffractions of complexes **1** (a)−**4** (d).

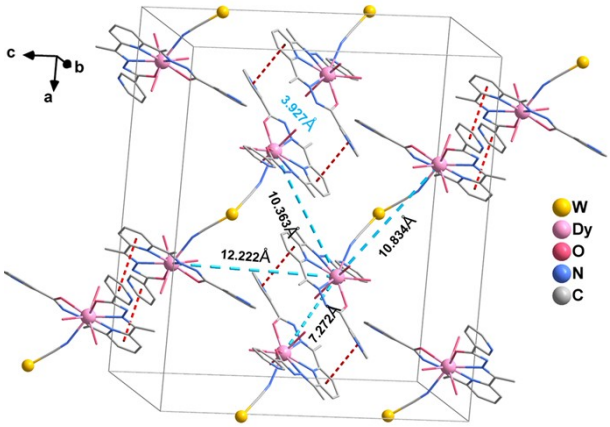

Fig. S3 π···π stacking interactions between pyridyl rings and the inter/intra-molecular Dy···Dy distances of complex **1** are presented as red and blue dotted lines. Hydrogen atoms, uncoordinated solvent molecules, and terminal cyano groups are omitted for clarity.

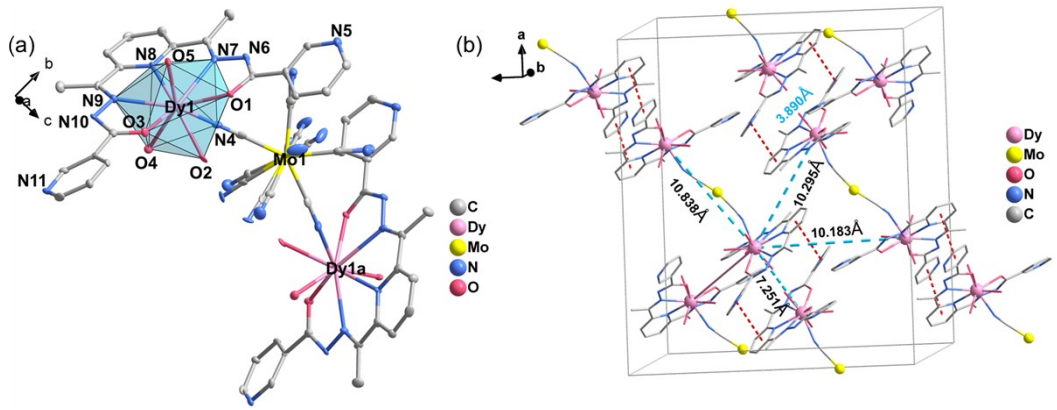

Fig. S4 (a) Ellipsoid plot of the trinuclear structure of **2**. Displacement ellipsoids are drawn at the 30% probability level. (b) π···π stacking interactions between pyridyl rings and the inter/intra-molecular Dy···Dy distances of complex **2** are presented as red and blue dotted lines. Hydrogen atoms, uncoordinated solvent molecules, and terminal cyano groups are omitted for clarity.

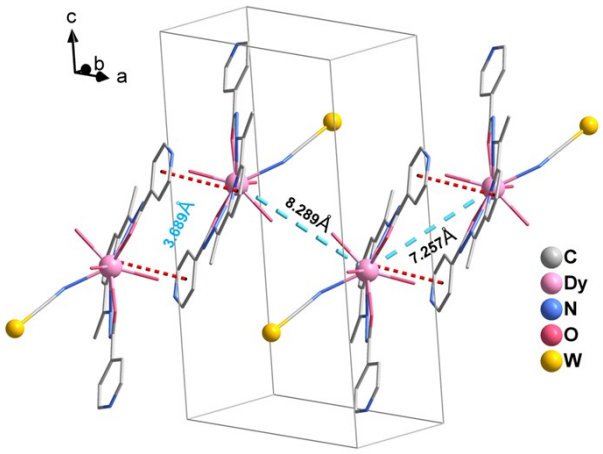

Fig. S5 π···π stacking interactions between pyridyl rings and the inter/intra-molecular Dy···Dy distances of complex **3** are presented as red and blue dotted lines. Hydrogen atoms, uncoordinated solvent molecules, and terminal cyano groups are omitted for clarity.

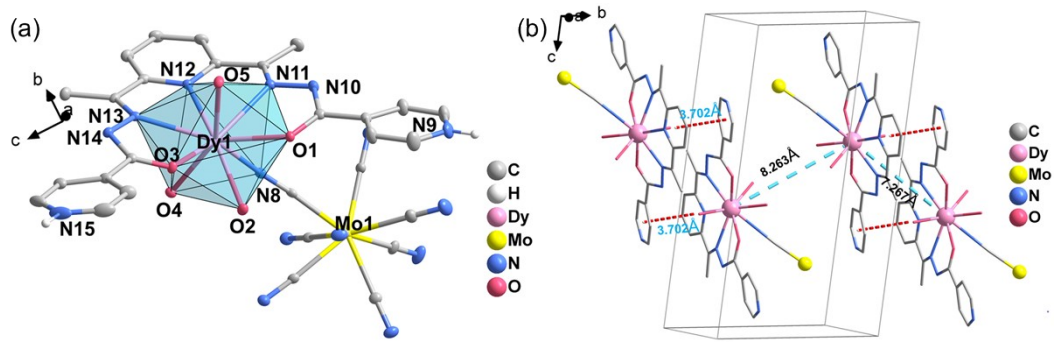

Fig. S6 (a) Ellipsoid plot of the trinuclear structure of **4**. Displacement ellipsoids are drawn at the 30% probability level. (b) π···π stacking interactions between pyridyl rings and the inter/intra-molecular Dy···Dy distances of complex **4** are presented as red and blue dotted lines. Hydrogen atoms, uncoordinated solvent molecules, and terminal cyano groups are omitted for clarity except for the protonated hydrogen atoms.

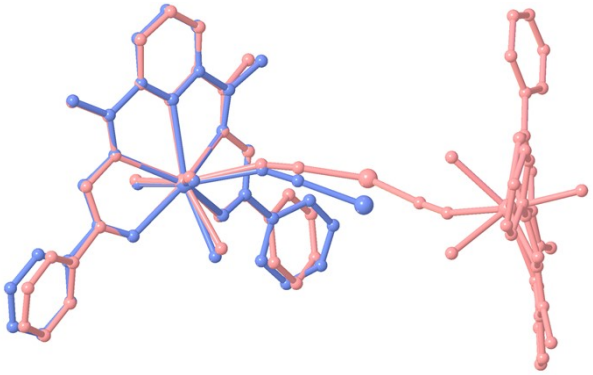

Fig. S7 Superposition plot of complexes **1** and **3**.

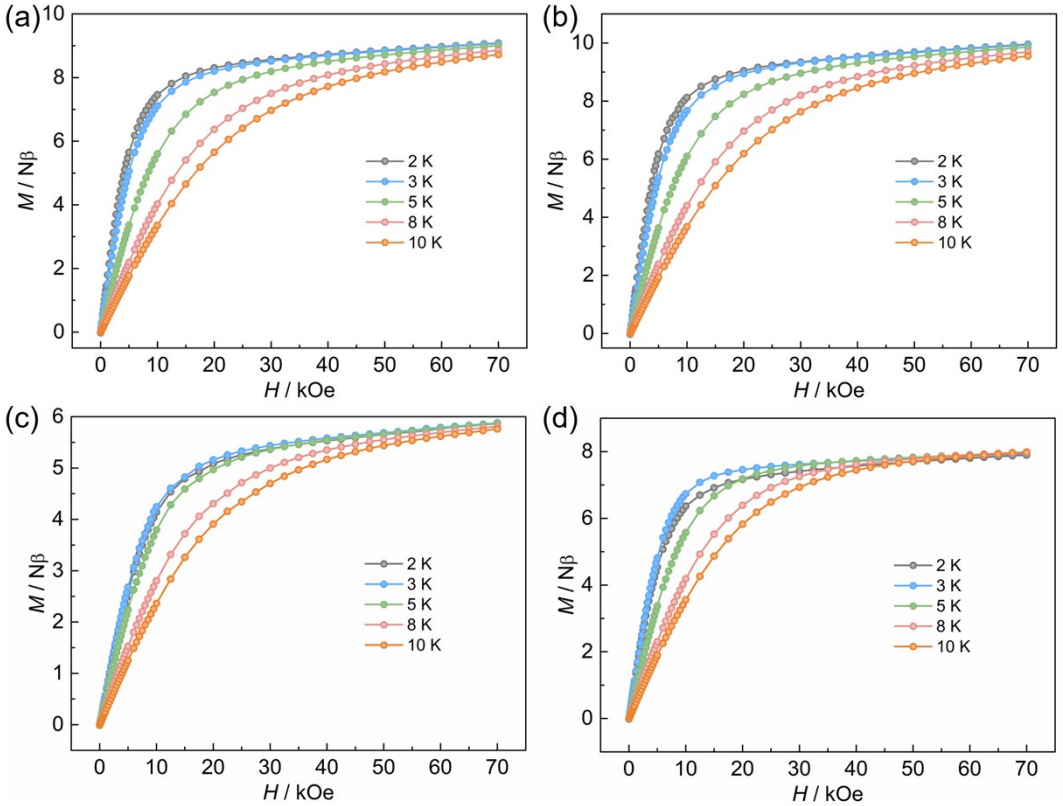

Fig. S8 The field dependence of the reduced magnetization at the indicated temperatures for **1** (a)−**4** (d).

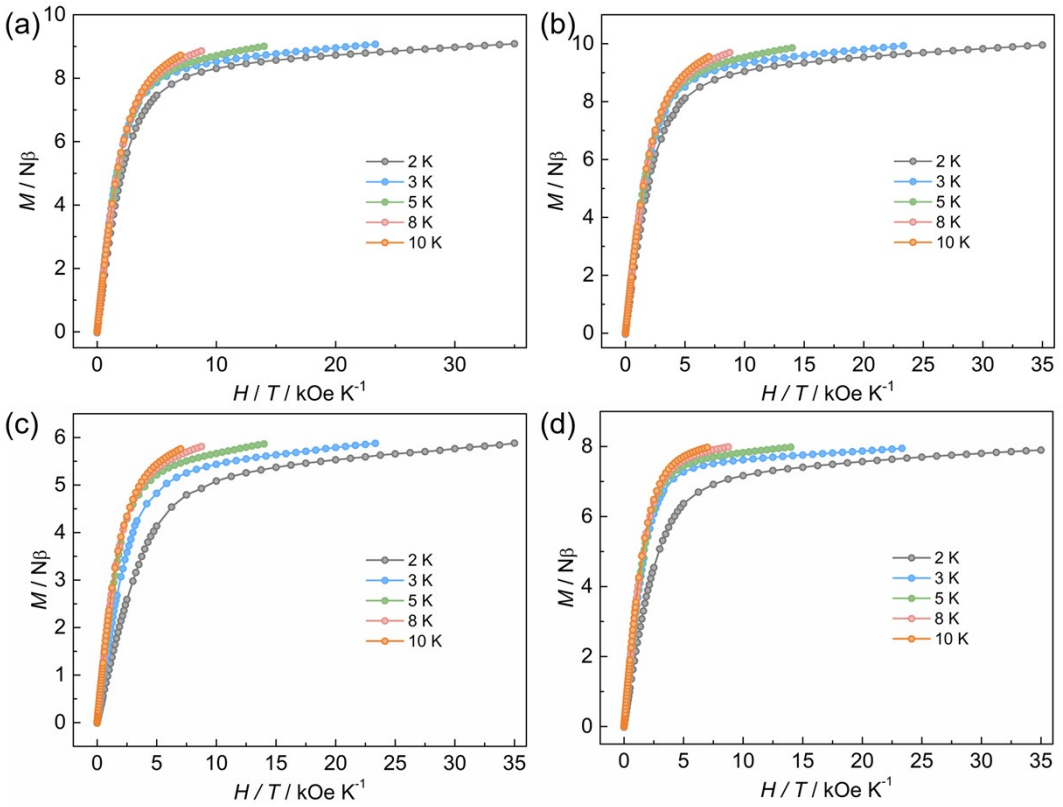

Fig. S9 The *M* vs. *H/T* plots for **1** (a)−**4** (d).

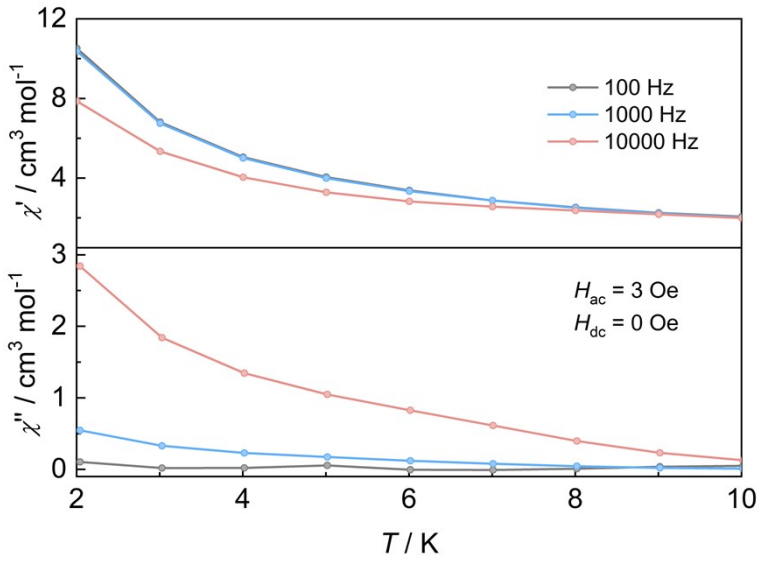

Fig. S10 Temperature dependences of ac magnetic susceptibilities for **1** under zero dc field.

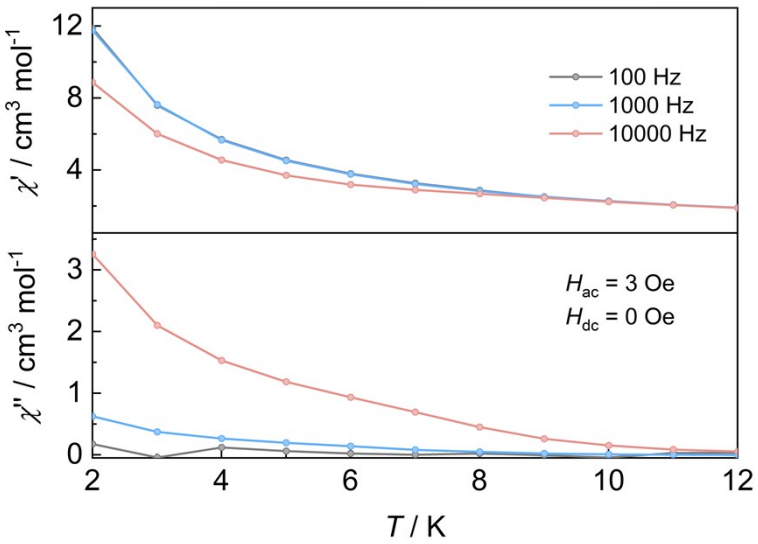

Fig. S11 Temperature dependences of ac magnetic susceptibilities for **2** under zero dc field.

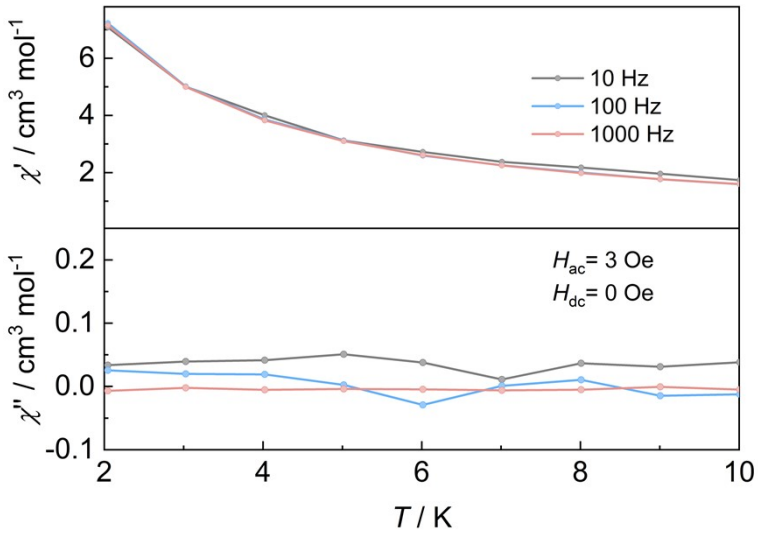

Fig. S12 Temperature dependences of ac magnetic susceptibilities for **3** under zero dc field.

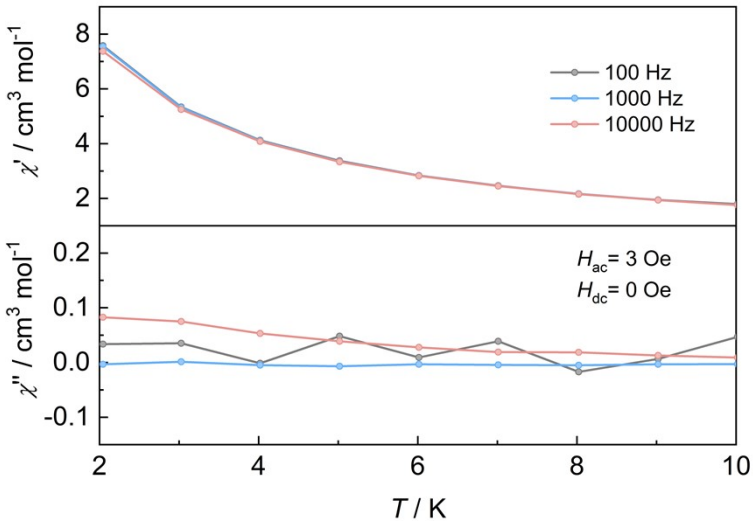

Fig. S13 Temperature dependences of ac magnetic susceptibilities for **4** under zero dc field.

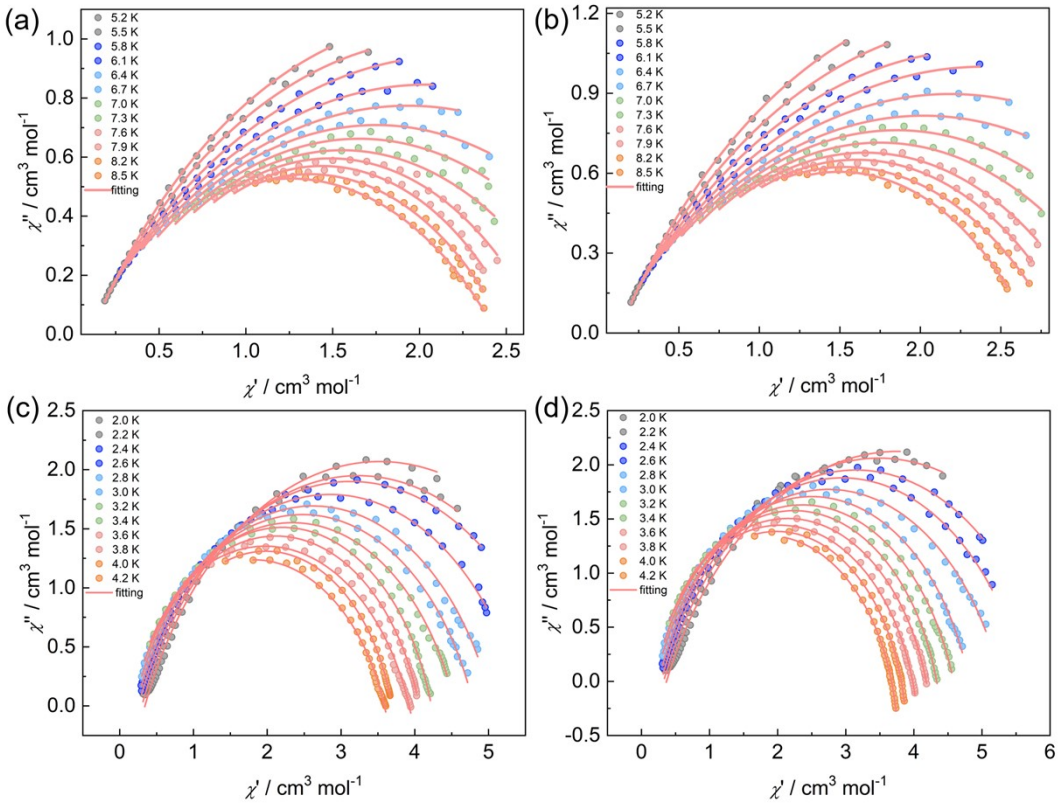

Fig. S14 Argand plots for **1** (a), **2** (b), **3** (c), and **4** (d). The solid lines indicate the fits to the Debye functions.

Computational details

Complexes **1** and **2** have one type of magnetic center Dy^{III} ion, but their structures are not central symmetric. Complete-active-space self-consistent field (CASSCF) calculations on individual Dy^{III} fragments for complexes **1**–**2** (see Fig. S15 for the calculated structures of **1**–**4**) on the basis of single-crystal X-ray determined geometry have been carried out with the OpenMolcas[S1] program package. Each individual Dy^{III} fragment in **1**–**2** was calculated keeping the experimentally determined structure of the corresponding compound while replacing the neighboring Dy^{III} ion by diamagnetic Lu^{III}.

The basis sets for all atoms are atomic natural orbitals from the OpenMolcas ANO-RCC library: ANO-RCC-VTZP for Dy^{III}; VTZ for close O and N; VDZ for distant atoms. The calculations employed the second order Douglas-Kroll-Hess Hamiltonian, where scalar relativistic contractions were taken into account in the basis set and the spin-orbit couplings were handled separately in the restricted active space state interaction (RASSI-SO) procedure.[S2–S3] Active electrons in 7 active orbitals include all *f* electrons (CAS (9 in 7) in the CASSCF calculation. To exclude all the doubts, we calculated all the roots in the active space. We have mixed the maximum number of spin-free state which was possible with our hardware (all from 21 sextets, 128 from 224 quadruplets, 130 from 490 doublets for Dy^{III}. The SINGLE_ANISO[S4–S6] program was used to obtain the energy levels, ***g*** tensors, magnetic axes, *et al.* based on the above CASSCF/RASSI-SO calculations.

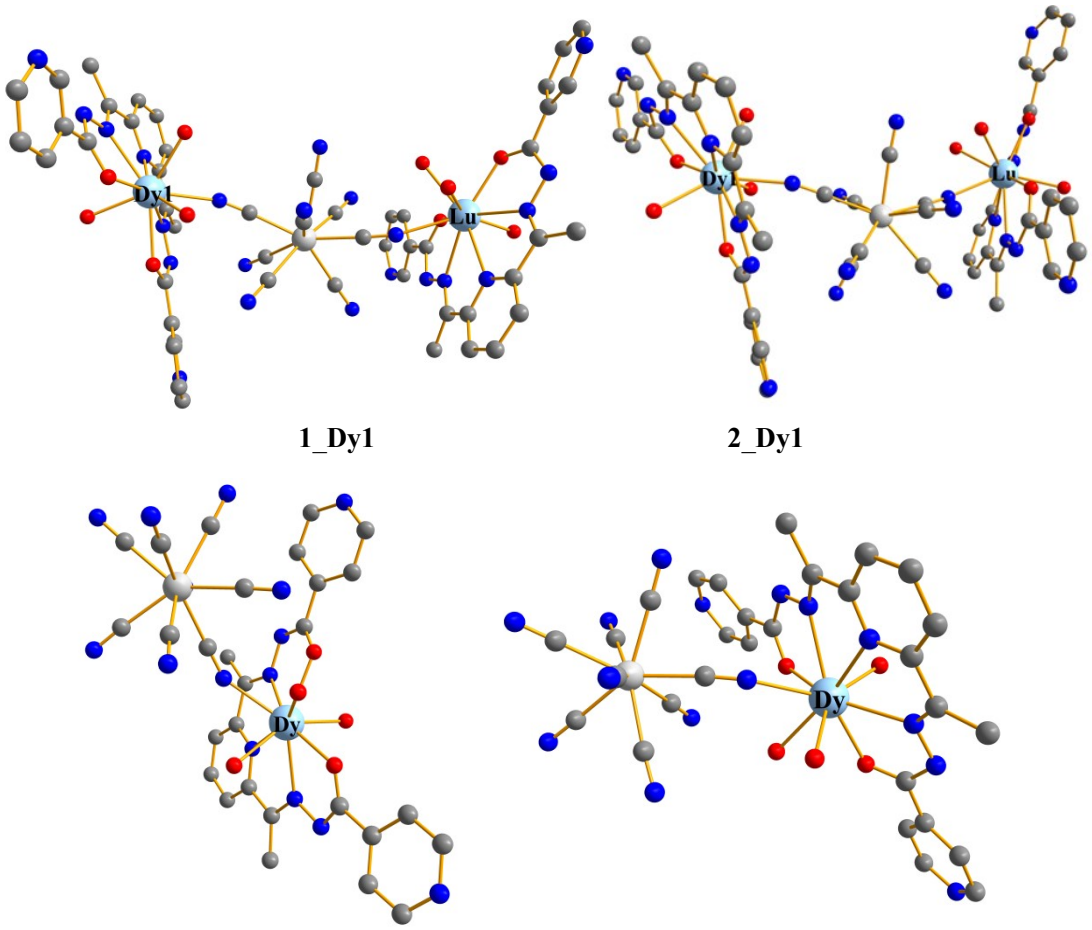

1_Dy1 **2_Dy1**

3 **4**

Fig. S15 Calculated structures of complexes **1_Dy1**, **2_Dy1**, **3**, and **4**. H atoms are omitted for clarity.

Table S8. Calculated energy levels (cm^{-1}), $\boldsymbol{g}$ (g_x, g_y, g_z) tensors, and predominant m_J values of the lowest eight Kramers doublets (KDs) of individual Dy^{III} fragments of complexes **1**−**4** using CASSCF/RASSI-SO with OpenMolcas.

KDs	**1_Dy1**			**2_Dy1**		
	E	***g***	m_J	*E*	***g***	m_J
1	0.0	0.010 0.018 19.618	±15/2	0.0	0.005 0.011 19.682	±15/2
2	153.9	0.289 0.617 16.726	±13/2	167.3	0.290 0.577 16.390	±13/2
3	226.6	1.965 2.555 14.496	±9/2	241.7	0.883 1.126 13.548	±11/2
4	265.6	1.185 3.133 11.337	±11/2	303.1	0.363 2.381 11.406	±9/2
5	333.6	9.287 6.147 1.567	±9/2	375.7	1.105 4.702 8.952	±7/2
6	386.7	2.724 4.742 11.275	±7/2	434.7	3.138 5.107 9.488	±1/2
7	427.8	1.313 2.412 17.286	±1/2	474.6	1.414 3.040 16.255	±3/2
8	594.8	0.016 0.029 19.576	±1/2	662.0	0.012 0.019 19.570	±1/2
KDs	**3**			**4**		
	E	***g***	m_J	*E*	***g***	m_J
1	0.0	0.002 0.030 19.554	±15/2	0.0	0.007 0.027 19.552	±15/2
2	118.4	1.111 2.506 15.401	±13/2	124.6	1.174 2.941 15.067	±13/2
3	159.5	1.350 3.349 12.445	±9/2	163.3	1.753 3.670 12.072	±9/2

4	201.4	8.976 5.293 1.017	±11/2	202.5	2.585 4.771 8.838	±9/2
5	270.2	0.636 4.418 9.191	±5/2	269.8	1.678 5.101 10.090	±7/2
6	319.1	9.380 6.505 3.192	±1/2	322.6	9.038 5.056 0.480	±1/2
7	359.7	1.209 2.147 17.815	±5/2	349.7	2.009 5.466 14.308	±3/2
8	484.7	0.033 0.049 19.295	±1/2	515.2	0.015 0.023 19.457	±1/2

Table S9. Wave functions with definite projection of the total moment | m_J > for the lowest eight KDs of individual Dy^{III} fragments for complexes **1**−**4** using CASSCF/RASSI-SO with OpenMolcas.

	E/cm^{-1}	wave functions
1_Dy1	0.0	96.6%|±15/2>
	153.9	69.1%|±13/2>+15.1%|±11/2>+8%|±7/2>
	226.6	27.2%|±9/2>+25.4%|±11/2>+14.8%|±7/2>+13%|±5/2>+9.5%|±13/2>+7.7%|±3/2>
	265.6	28.8%|±11/2>+19.1%|±9/2>+18.7%|±13/2>+13.6%|±5/2>+11.6%|±7/2>
	333.6	28.5%|±9/2>+22.9%|±11/2>+19.5%|±3/2>+19.3%|±7/2>
	386.7	25.5%|±7/2>+23.3%|±5/2>+22.8%|±1/2>+12.7%|±9/2>+9.6%|±3/2>
	427.8	34.8%|±1/2>+29.9%|±3/2>+21.5%|±5/2>+9.2%|±7/2>
	594.8	30.4%|±1/2>+29.7%|±3/2>+21.6%|±5/2>+11.4%|±7/2>
2_Dy1	0.0	97.6%|±15/2>
	167.3	79.5%|±13/2>+10.8%|±11/2>+6.1%|±7/2>
	241.7	47.1%|±11/2>+25.6%|±9/2>+8.6%|±7/2>+7.6%|±13/2>+7.1%|±5/2>
	303.1	31.1%|±9/2>+20.7%|±11/2>+16.9%|±7/2>+14.7%|±5/2>+9.6%|±13/2>
	375.7	28.4%|±7/2>+22.3%|±3/2>+22.1%|±9/2>+13.6%|±11/2>+8.2%|±5/2>
	434.7	31.2%|±1/2>+27.6%|±5/2>+18.7%|±7/2>+10.2%|±9/2>+6%|±3/2>
	474.6	35.6%|±3/2>+27.6%|±1/2>+20.4%|±5/2>+10.5%|±7/2>
	662.0	33.8%|±1/2>+29.4%|±3/2>+19.9%|±5/2>+10.4%|±7/2>
3	0.0	96%|±15/2>
	118.4	66.2%|±13/2>+17.8%|±11/2>+6.6%|±5/2>
	159.5	32.2%|±9/2>+25.8%|±11/2>+12.5%|±13/2>+10.6%|±13/2>+9.3%|±3/2>
	201.4	22.9%|±11/2>+22.6%|±9/2>+22.1%|±7/2>+9.7%|±5/2>+9.5%|±13/2>+8.9%|±1/2>
	270.2	24.9%|±5/2>+19.5%|±7/2>+14.8%|±3/2>+13.4%|±9/2>+11.1%|±11/2>+9.4%|±1/2>
	319.1	30.8%|±1/2>+25.2%|±3/2>+11.5%|±7/2>+11.2%|±11/2>+10.6%|±9/2>+8%|±5/2>
	359.7	23.2%|±5/2>+19.2%|±1/2>+18.5%|±3/2>+17.2%|±7/2>+11.7%|±9/2>+6.1%|±11/2>
	484.7	29.6%|±1/2>+26.7%|±3/2>+19.8%|±5/2>+11.9%|±7/2>+7.2%|±9/2>
4	0.0	95.7%|±15/2>
	124.6	61.6%|±13/2>+16.6%|±11/2>+8.3%|±7/2>+7.7%|±5/2>
	163.3	28%|±9/2>+26.4%|±11/2>+15.2%|±13/2>+12.8%|±7/2>+8.9%|±3/2>

	202.5	29.5%|±9/2>+20.6%|±11/2>+15%|±7/2>+12.5%|±13/2>+11.9%|±5/2>+7.4%|±1/2>
	269.8	24.9%|±7/2>+18.8%|±5/2>+18.3%|±3/2>+12.1%|±11/2>+10.3%|±9/2>+9.1%|±1/2>
	322.6	36%|±1/2>+15.5%|±3/2>+15.5%|±11/2>+11.9%|±5/2>+10.5%|±7/2>+8%|±9/2>
	349.7	25.5%|±3/2>+23.9%|±5/2>+15.6%|±7/2>+14.4%|±9/2>+13.3%|±1/2>
	515.2	30.8%|±1/2>+26.5%|±3/2>+19.5%|±5/2>+12.2%|±7/2>+6.9%|±9/2>

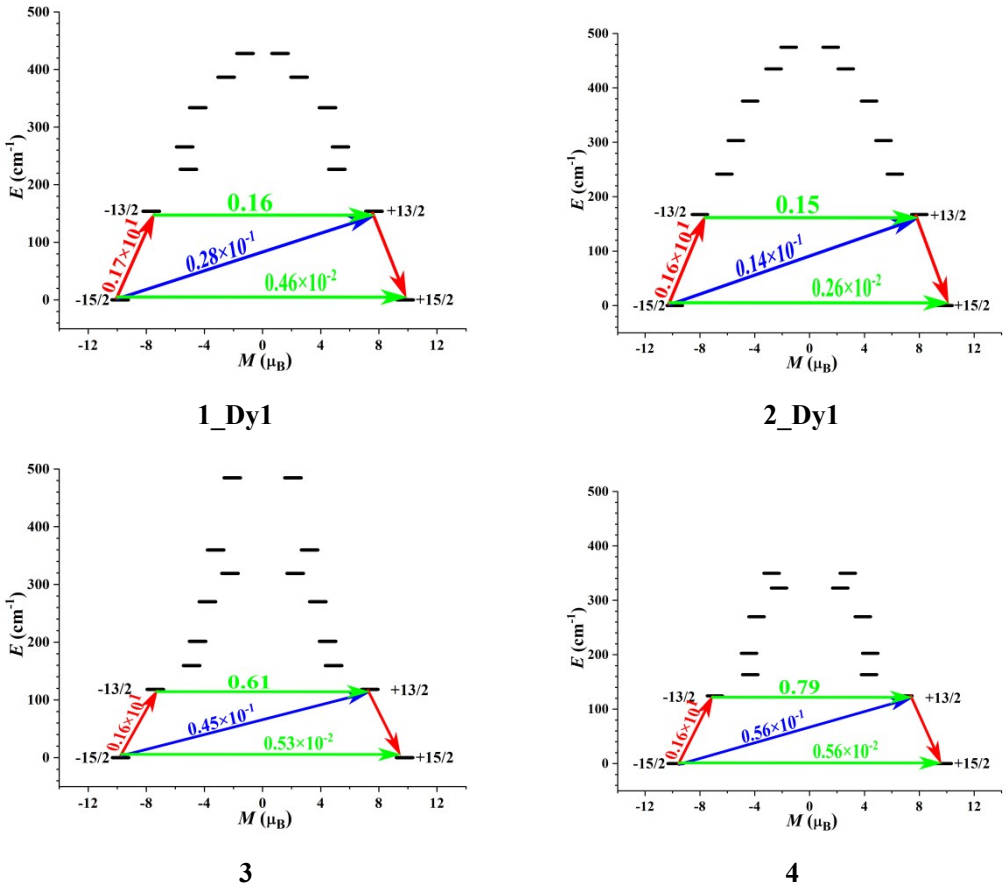

Fig. S16 Magnetization blocking barriers of individual Dy^{III} fragments for **1**–**4**. The thick black lines represent the KDs as a function of their magnetic moment along the magnetic axis. The green lines correspond to diagonal quantum tunneling of magnetization (QTM); the blue line represent off-diagonal relaxation process. The numbers at each arrow stand for the mean absolute value of the corresponding matrix element of transition magnetic moment.

References:

S1 I. F. Galván, M. Vacher, A. Alavi, C. Angeli, F. Aquilante, J. Autschbach, J. J. Bao, S. I. Bokarev, N. A. Bogdanov, R. K. Carlson, L. F. Chibotaru, J. Creutzberg, N. Dattani, M. G. Delcey, S. S. Dong, A. Dreuw, L. Freitag, L. M. Frutos, L. Gagliardi, F. Gendron, A. Giussani, L. González, G. Grell, M. Guo, C. E. Hoyer, M. Johansson, S. Keller, S. Knecht, G. Kovačević, E. Källman, G. L. Manni, M. Lundberg, Y. J. Ma, S. Mai, J. P. Malhado, P. Å. Malmqvist, P. Marquetand, S. A. Mewes, J. Norell, M. Olivucci, M. Oppel, Q. M. Phung, K. Pierloot, F. Plasser, M. Reiher, A. M. Sand, I. Schapiro, P. Sharma, C. J. Stein, L. K. Sørensen, D. G. Truhlar, M. Ugandi, L. Ungur, A. Valentini, S. Vancoillie, V. Veryazov, O. Weser, T. A. Wesołowski, P. O. Widmark, S. Wouters, A. Zech, J. P. Zobel and R. Lindh, *J. Chem. Theory Comput.*, 2019, **15**, 5925−5964.

S2 P. Å. Malmqvist, B. O. Roos and B. Schimmelpfennig, *Chem. Phys. Lett.*, 2002, **357**, 230−240.

S3 B. A. Heß, C. M. Marian, U. Wahlgren and O. Gropen, *Chem. Phys. Lett.*, 1996, **251**, 365−371.

S4 L. F. Chibotaru, L. Ungur and A. Soncini, *Angew. Chem., Int. Ed.*, 2008, **47**, 4126−4129.

S5 L. Ungur, W. Van den Heuvel and L. F. Chibotaru, *New J. Chem.*, 2009, **33**, 1224−1230.

S6 L. F. Chibotaru, L. Ungur, C. Aronica, H. Elmoll, G. Pilet and D. Luneau, *J. Am. Chem. Soc.*, 2008, **130**, 12445–12455.

S7 M. E. Lines, *J. Chem. Phys*., 1971, **55**, 2977−2984.

S8 K. C. Mondal, A. Sundt, Y. Lan, G. E. Kostakis, O. Waldmann, L. Ungur, L. F. Chibotaru, C. E. Anson and A. K. Powell, *Angew. Chem., Int. Ed.*, 2012, **51**, 7550−7554.

S9 S. K. Langley, D. P. Wielechowski, V. Vieru, N. F. Chilton, B. Moubaraki, B. F. Abrahams, L. F. Chibotaru and K. S. Murray, *Angew. Chem., Int. Ed.*, 2013, **52**, 12014−12019.